International Journal of Electrical Engineering and Technology.
ISSN 2249-3085 Volume 12, Number 1 (2022), pp. 1-16

http://www.ripublication.com

Electric Field Analysis of 11 kV Nano Filled Silicon Rubber Insulators

Sunanda C

Deprtment of electrical and Electronics Engineering, Rashtreeya Vidyalaya College of Engineering, Banglore 560059, Karnataka, India.

Dr. G.S. Sheshadri

Deprtment of Electrical and Electronics Engineering, SSIT,Tumkur-572107, Karnataka, India.

Dr. M.N. Dinesh

Deprtment of Electrical and Electronics Engineering Rashtreeya Vidyalaya College of Engineering Banglore 560059, Karnataka, India

Abstract

Insulators are very important part of power system. They provide an insulation between ground and phases. Polymer insulators are very popular in these days because of their light weight, hydrophobicity, good UV radiation and high elasticity. In adverse environmental conditions fog, rain droplets along with dust on the surface of an insulator will form conduction layer. Which is resulted in a leakage current start flowing through an insulator which leads to flashover which is a failure of insulator. Hence in simulated environment the polymer insulator is tested using CAD and ANSYS software to find the electric distribution, electric flux density and electric potential along a sheath and shed area of a composite insulators in with different composition and in different pollution level. There by obtaining a leakage current at various level of pollution.

Keywords: Polymer insulator, electric field, electric potential, electric flux density.

I. INTRODUCTION

The Insulator is the most commonly used device in the power system. It provides isolation from the ground as well as from other phases or circuits. Insulators are

classified into three types: Porcelain Insulators, glass Insulators and Composite Insulators. Polymer Insulators are increasingly being employed for outdoor applications, have superior properties over porcelain and glass Insulators. They have several advantages over porcelain Insulators. They work well in contaminated environments, have excellent mechanical strength, require little maintenance, they are small in weight and have low maintenance costs. Electrical insulation failure is one of the leading causes of power outages in most types of electrical power equipment. Many research is being conducted to increase the service life and minimize early failure of electrical systems by improving the electrical insulation systems in use or reducing the electrical stress. A range of factors influences electrical distribution, including the geometry of the Insulator, the geometry of the attachment hardware, the magnitude of the energized line voltage and the presence of nearby phases [1][3].

The pattern of Potential and Electric Fields on the Insulator surface are exceedingly rough. The strongest Electric Field is found at the joint of the rod, silicon rubber and end fitting, while the first shed has the most excellent distributed voltage. Sealing points have a strong Electric Field strength and a high valued electric stress that may quickly erode it, producing flashovers and mechanical failures. Once the Electric Field on the Composite Insulator and end fitting surface exceed the allowable value, the Corona phenomenon occurs, altering the electromagnetic conditions of power transmission lines and the insulation material qualities [7]. The distribution of Electric Fields on Composite Insulators influences both long term and short term performance. Long term discharge on silicon rubber surfaces accelerates rubber aging and may even cause ablation, reducing service life of Composite Insulator. As a result, analyzing the Electric Field distribution of the Composite Insulator in the presence of surface pollution is critical [10]. The Electric Field along the length is intensified in moist and dirty conditions, resulting in flashover. In service Insulator, flashover could result in power supply outages, affecting the reliability of the bulk systems. The effect of water droplets on the distribution of an electrical field has been analysed in several studies [8].

II. CAD MODELLING

A. CAD Model Development

The design of the CAD model is developed in CATIA software according to IS: 731 standard dimensions, as shown in Table 1

Table 1: Insulator Dimensions

Insulator Dimensions	
Creepage distance	216mm
Trunk diameter	19mm
FRP ROD Diameter	16mm
FRP ROD Length	200mm
No of sheds	3
Shed diameter	58mm
Dry arc Distance	118mm

A. 3D view of 11kV polymer insulator is shown in Figure 1.

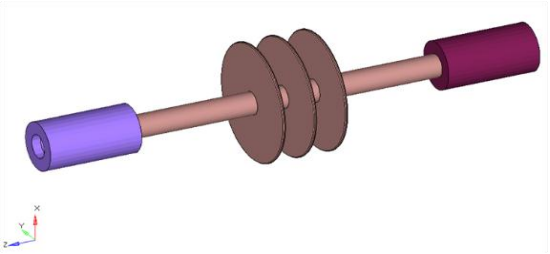

Figure 1. CAD Model of 11kV Polymer insulator

B. Calculation of Pollution Concentration

Sodium chloride solution is used as pollutant. The chemical formula for sodium chloride is NaCl, having molecular mass of 58.44276 kg/mol. Sodium reacts with chloride gas to form a sodium chloride. During this reaction only one electron is transferred.

$$2Na(s) + Cl_2(g) \longrightarrow 2NaCl(s)$$

The pollution concentration of different pollution levels are listed in the table 2.

Table 2. Different Pollution Level Concentration

Pollution level	Concentration (kg/m^3)	Concentration in Normality (g/l)	Relative permittivity
Low pollution	8(kg/m^3)	0.06844 Mol/l	80
Medium pollution	4(kg/m^3)	0.1368 Mol/l	78
High pollution	12(kg/m^3)	0.205 Mol/l	76

C. Meshing of the insulator

Meshing is made onto the CAD model of 11kV insulator for finite element analysis. Figure 2 shows the meshing of the insulator using HyperMesh. The model is placed under air-domain to depict the real world scenario the Figure 3

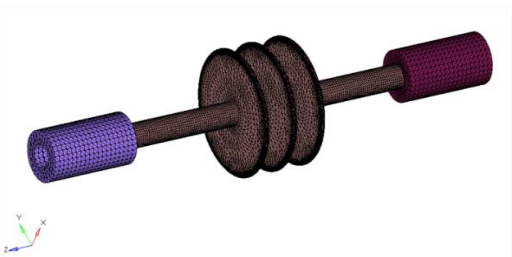

Figure 2. Meshing of insulator

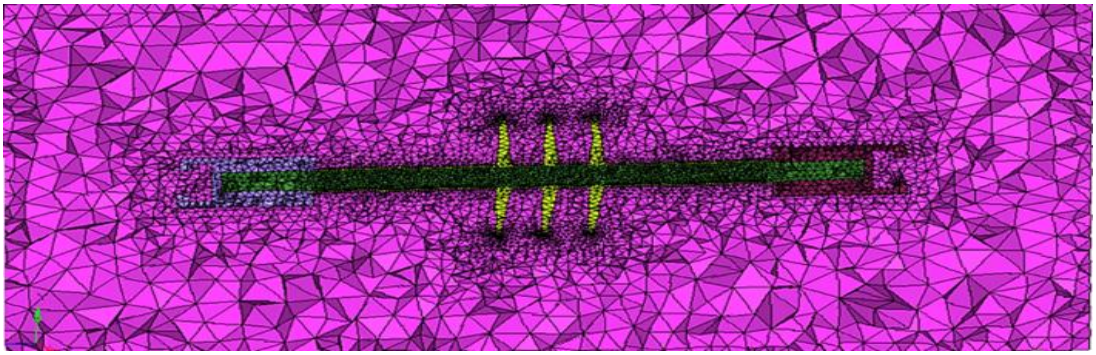

Figure 3. Insulator under air-domain

III. ANALYSIS OF INSULATOR USING APDL

The 11kV silicon rubber insulator model is meshed by using HyperMesh software imported to APDL multiphysics. In preferences, choose both structural and electrical analysis as this work involves analyzing both mechanical and electrical findings. a silicon rubber based polymer insulator with varying compositions of MgO nanofillers by weight 5%,7.5% and 10% at different pollution levels is simulated. This is performed by changing the relative permittivity.

A. Mechanical properties

The mechanical properties are given to insulator to perform mechanical displacement and stress test. Table 3 list the mechanical properties of insulator.

Table 3. Mechanical Properties of Insulator

Material Properties			
Properties	**SiR**	**FRP**	**Cast Iron**
Youngs modulus	0.208Gpa	0.024Gpa	92.4Gpa
Paisson's Ratio	0.5	0.1	0.27
Density	1.24g/cc	1.857g/cc	7.20g/cc
Yield Strength	10.5Mpa	3450Mpa	344.73Mpa

B. Electrical properties

The Silicon Rubber is used as pure silicon rubber ,to that Magnesium Oxide is added in percentage to enhance the electrical properties of insulator, hence to increase the lifespan of the insulator. Tan delta measurements are used to calculate the amount of real power dissipation and quality of insulator in a dielectric material. Tan delta and relative permittivity of silicon rubber insulator with varying MgO nanofiller composition is shown in Table 4.

Table 4. Electrical properties of silicon rubber

Material Composition	Tan Delta	Dielectric Constant
SIR+10% MgO	0.07473	4.76
SIR+7.5% MgO	0.07965	4.88
SIR+5% MgO	0.07465	4.68
Silicone Rub	0.0611	4.38

C. Boundary Conditions

The HV terminal is set to 11kV, whereas the ground terminal is set to 0V, as shown in Figure 3. The air is created large enough to have no effect on the distribution of the electric field along the insulator at both the terminals. The air background region's outer edges are assumed to have zero external current.

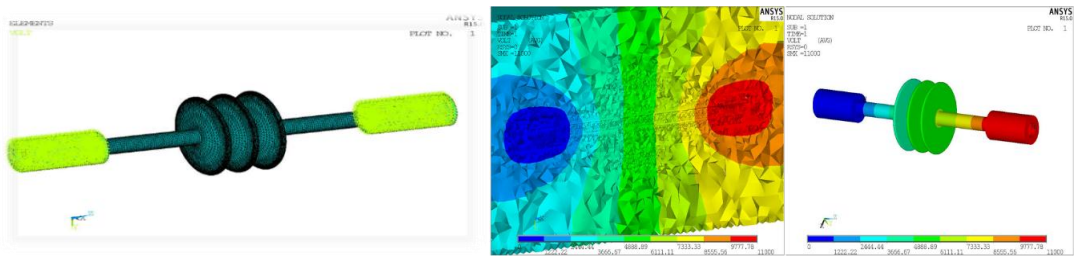

Figure 4. Implementation of Boundary on the Insulator

D. Mechanical displacment Simulation

The Mechanical displacement is obtained by applying the properties from table II.

The change in mechanical displacement for a 45kN load is shown in Figure 5. At the live end, there is a large displacement of 32mm, whereas at the ground end, there is no displacement.

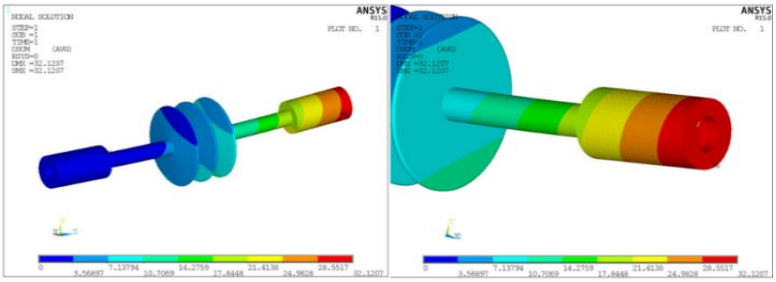

Figure 5. Mechanical Displacement change in 11kV Insulator

E. Mechanical Stress Simulation

The mechanical stress at various sections of the insulator is shown in Figure 6, with the highest stress at the FRP rod and the lowest stress at the shed and metal fitting.

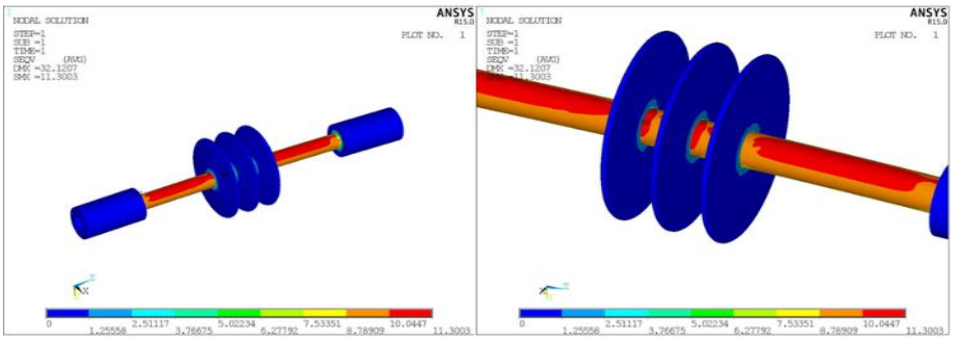

Figure 6. Mechanical Stress at Various Part of Insulator

F. Electrical Potenital Simulation

The electric potential is depicted in Figure 7 presents the insulator without pollution layer that is placed in air medium and Figure 8 shows the impact of electric potential with pollution layer. The value of the corresponding colour is shown by the stripe in the Figures. The voltage is about 11kV at the live end and zero at the ground end.

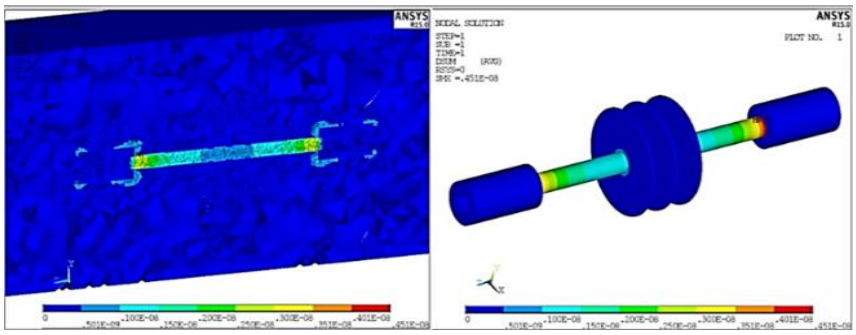

Figure 7. Electric Potential of 11kV Insulator Without Pollution Layer

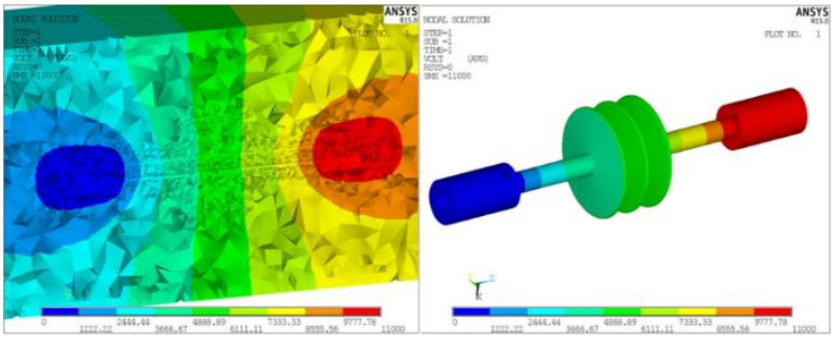

Figure 8. Electric Potential of Insulator with Pollution Layer

G. Electric Field Simulation

The electric field distribution along the insulator that include a 3D model under air medium and sectional Figure of the insulator. The electric field is high at the connection between the FRP rod and metal fitting. The Figure 9 represents impact of electric field on insulator without pollution layer and Figure 10 shows impact of electric field with pollution layer.

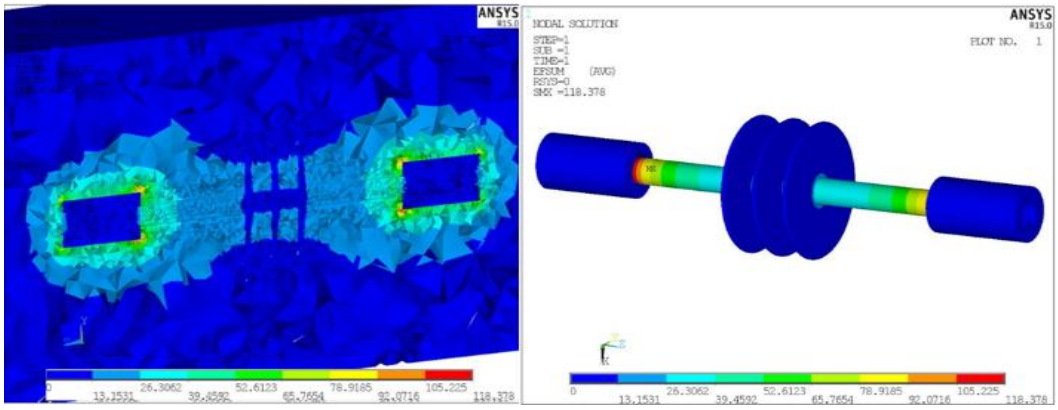

Figure 9. Electric Field of Insulator Without Pollution Layer

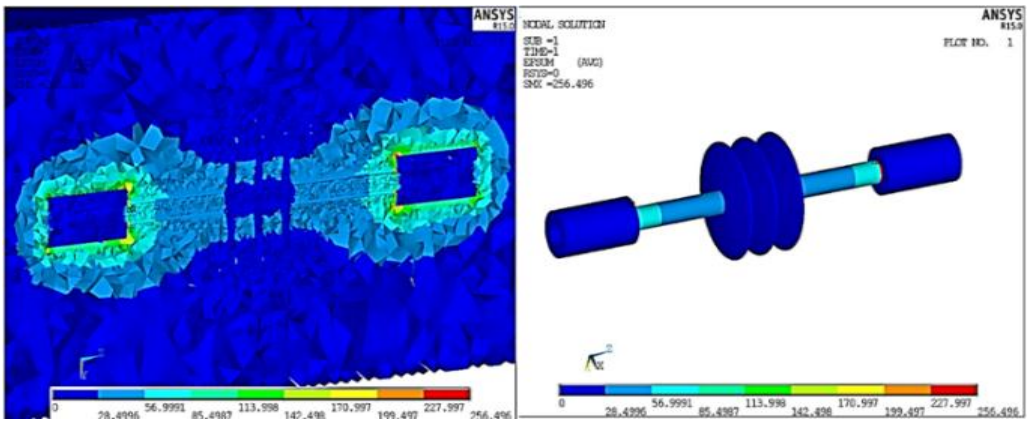

Figure 10. Electric Field of Insulator with Pollution Layer

H. Electrical Flux Density

As electric flux density is compared with and without pollution layer, the flux at the metal fitting and shed is minimal. The Figure 11 illustrates the impact of electric flux density on insulator without pollution layer and Figure 12 shows impact of electric flux density with pollution layer.

Figure 11. Electric Flux Density of Insulator Without Pollution Layer

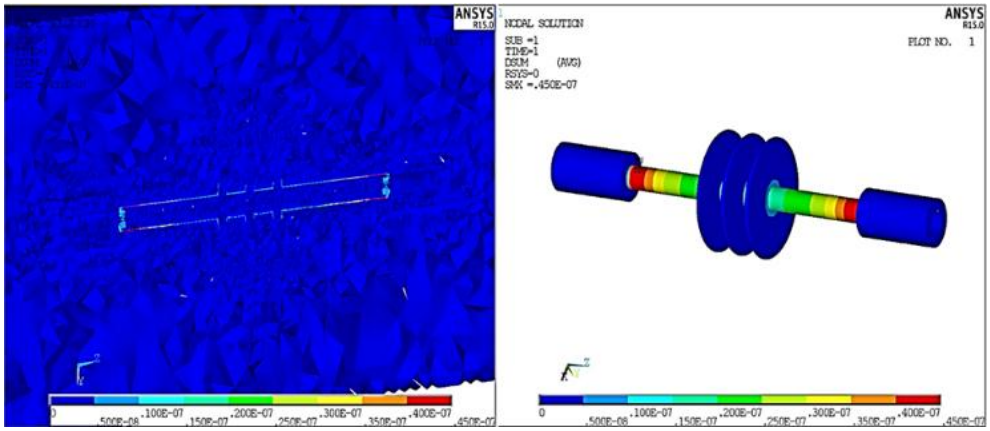

Figure 12. Electric Flux Density of Insulator with Pollution Layer

IV. GRAPHICAL COMPARISON OF RESULTS

The simulation/graphical results of electric field, electric flux density, mechanical displacement and stress of an insulator with and without pollution layer are compared. It discusses the result and compares with different pollution levels and leakage current calculation.

A. Mechanical Load Displacement

The mechanical load displacement of the 11kV insulator is performed by using a 45kN load on the line and the ground end is fixed. The tension at the top end is high compared to the ground end. The simulated result shows about 32.12mm displacement at the metal fitting of the live end. At the ground end side, displacement is zero because it is rigidly fixed and there is no net load acting on it. The value of displacement starts to decrease from the live end to the ground end.

B. Mechanical Load Stress

A mechanical load stress analysis is performed by applying the tensile load of 45kN. Figure 6 shows that the stress is more at the FRP rod and connection between FRP rod and shed. This is due to the low value(0.024gpa) of young's modulus at FRP rod. The stress is minimum at the ground end, as these materials are cast iron with a high young's modulus of 92.4 gpa. The value of stress at the FRP rod is high as 11.303 gpa and a metal fitting has a low value of 0-1.2558 gpa.

C. Electrical potential

Ansys parametric design language is used for the simulation of electric potential by applying 11kV at the metal fitting and 0V at ground end metal fitting. The electric potential of 11kV insulator without pollution layer of different permittivity is compared with electric potential with pollution layer of 8kg/m^3 and has a relative permittivity of 78. The potential is high at the live end metal fitting, having a value of 11000V and the potential is minimum at the ground end metal fitting, having a value of 0V.

The electric potential at the shed has a value from 11000V-0V. Hence, With the different pollution layers, the change in the electric potential is negligible. There is a drop in the electric potential as distance rises.

There is less influence on the electric potential as compared to the insulator with a pollution layer. The Figure 13 compares the electric potential distribution for pure SIR insulator with and without pollution layer.

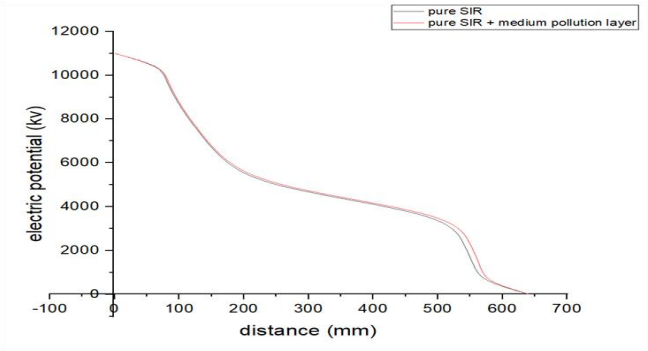

Figure 13. Electric Potential of pure SIR

There is negligible difference in electrical potential of varying composite insulator as compared to pure SIR Insulator. The electrical potential distribution of SIR along with MgO nanofiller as shown in Figure 14

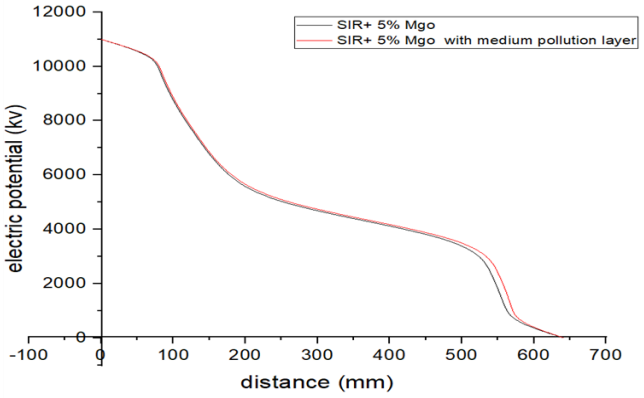

Figure 14. Electric Potential of SIR with MgO Nanofillers

D. Electrical Field Distibution

The electric field study is performed by applying 11kV at the metal fitting and simulated in APDL. The electric field distribution of 11kV insulator without pollution layer of different composition of nanofillers is compared with different pollution levels. The electric field is high at the connection between metal fitting and FRP rod due to transition from two different types of materials. Electric field is minimum at the weather sheds of insulators because of its high resistivity. The electric field intensity increases as pollution

severity increases. The electric field intensity decreases with an increase in relative permittivity of insulator composition. The electric field distribution of different compositions of insulators without pollution is shown in the Figure 15.

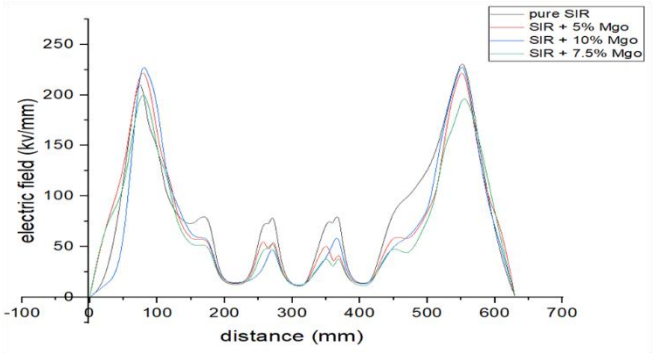

Figure 15. Electric Field of Insulator Without Pollution

Electric field intensity for different compositions of insulators with low pollution is slightly high as compared to without pollution layer. Electric field intensity of insulators with low pollution severity as shown in Figure 16.

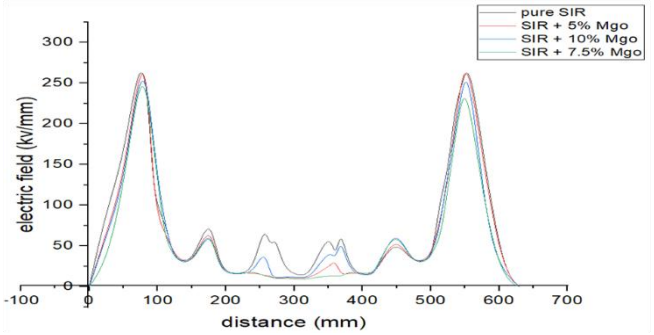

Figure 16. Electric Field of Insulator with Low Pollution

Electric field intensity for different composition of insulator with medium pollution as shown in the Figure 17.

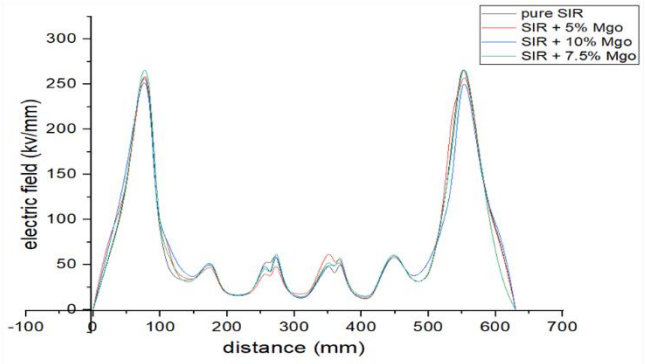

Figure 17. Electric Field of Insulator with Medium Pollution

Electric field intensity is more in high pollution severity as compared to medium and low pollution. Electric field distribution of insulators with high pollution is shown in Figure 18.

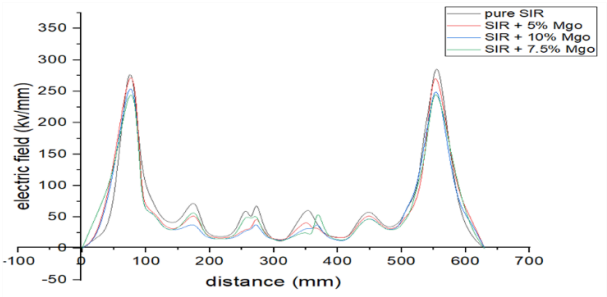

Figure 18. Electric Field of Insulator with High Pollution

Electric field is very high in metal fitting and FRP rod connection and its highest values are shown in Table 5.

Table 5. Maximum Electric Field

	Without pollution layer KV/mm	**With low Pollution** KV/mm	**With Medium pollution** KV/mm	**With High Pollution** KV/mm
Pure SiR	240.16	278.23	281.46	332.77
SiR+5% MgO	231.04	270.2	280	292.42
SiR+ 7.5% MgO	208.33	260	286.05	263.14
SiR + 10% MgO	237.08	265.46	269.55	278.64

E. Electric Flux Density

The Electric flux density for various compositions of insulators with varying severities of pollution is done by APDL Simulation. The graph of electric flux density is plotted with different relative permittivity of insulator and compared at various pollution levels. The electric flux density provides almost the same value for various compositions of nanofillers. Electric flux density without pollution is relatively more minor as compared to electric flux density with pollution. The electric flux density is high at the connection between metal fitting and FRP rod and the electric flux density is minimum at the weather sheds of insulators. The electric flux density of insulators without pollution is shown in Figure 18.

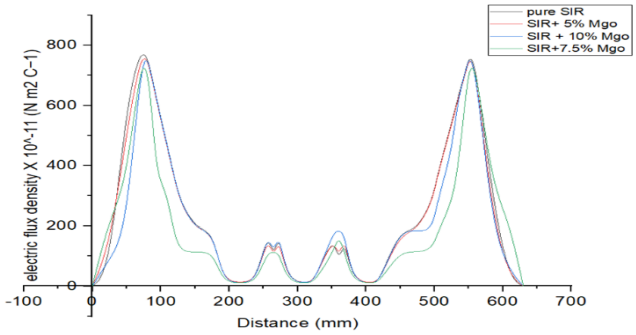

Figure 18. Electric Flux Density of Insulator Without Pollution

The electric flux density with low pollution as shown in the Figure 19. As observed the electric flux density is same for all composition of nanofillers

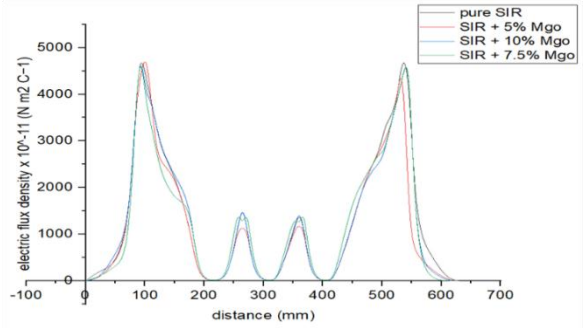

Figure 19. Electric Flux Density of Insulator with Low Pollution

The electric flux density for medium pollution as shown in the Figure 20.

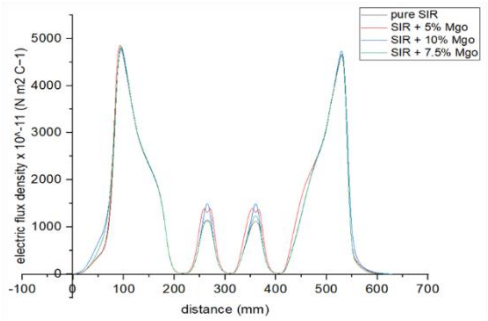

Figure 20. Electric Flux Density of Insulator with Medium Pollution

The electric flux density for different composition of nanofillers with high pollution as shown in the Figure 21. Electric flux density of different composition nanofiller is almost same.

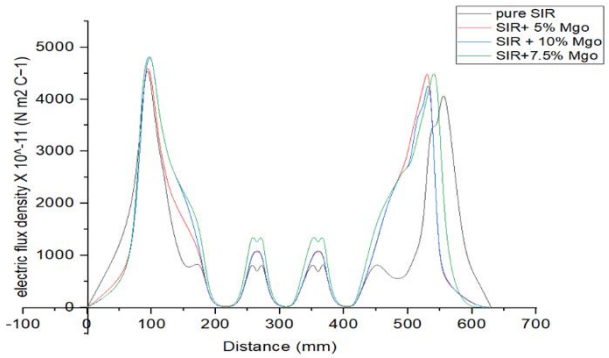

Figure 21. Electric Flux Density of Insulator with High Pollution

F. Leakage Current Analysis

Leakage current develops on insulators due to pollution, ageing of insulating materials and severe weather conditions. These currents produce line defects, such as flashover and degradation of the insulating material thus increases the conductivity of insulator.

The Table 6 shows Conductivity of Insulator for various dielectric constant.

Table 6. Conductivity of Insulator with Different Sample

Insulator Samples	**Conductivity Values**
Pure Silicon Rubber	$7.4301*10^{-10}$S/m
Sil Rubber +5% MgO	$9.7003*10^{-10}$S/m
Sil Rubber + 7.5% MgO	$10.778*10^{-10}$S/m
Sil Rubber + 10% MgO	$9.8645*10^{-10}$S/m

The Leakage current is calculated by the formula

Current density (J)= σ ×E.

Where, σ is conductivity: the value is considered from Table 6.

E is electric field along the polymer insulator.

The leakage current is obtained by integrating current density with a surficial area of the insulator. Leakage current along the surface of the insulator is equal **I=**$\int_s J.ds$.

Where, S is the surface area of insulator.

The Figure 21 shows leakage current at different parts of insulator.

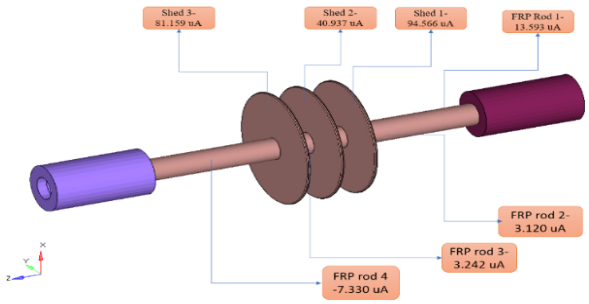

Figure 21. Leakage current of 11kV Insulator

By this method, leakage current for pure insulator and different amount of pollution layer is calculated and compared as shown in Table 7.

Table 7. Leakage current of Insulator with Different Pollution Level

	Low pollution in uA	**Medium pollution in uA**	**High pollution in uA**
Pure Silicon Rubber	207.86	235.852	243.979
Sil Rubber +5% MgO	290.186	314.326	344.224
Sil Rubber + 7.5% MgO	285.108	305.286	319.870
Sil Rubber + 10% MgO	265.10	274.982	285.158

The bar graph of leakage current with various pollution levels is shown in Figure 22. For pure silicon rubber, leakage current is minimal; once pollution levels increase, leakage current rises; however, as nanofiller content increases, leakage current decreases.

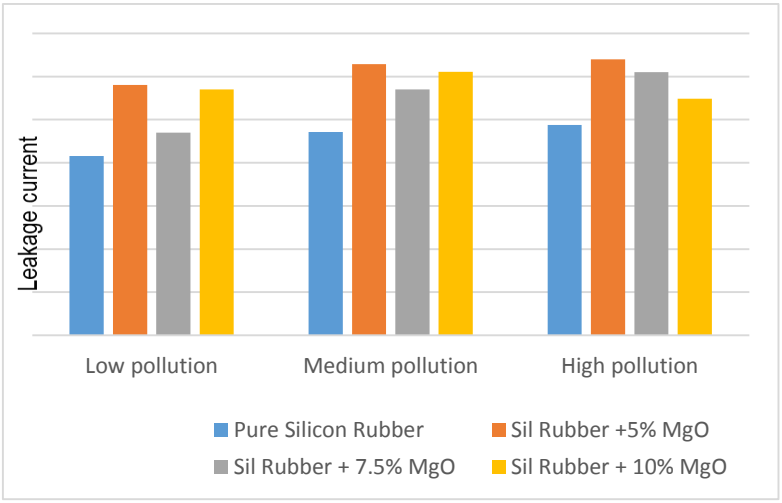

Figure 22. The bar graph of leakage current with various pollution levels

V. CONCLUSION

Mechanical load of 45kN is used to analyze the mechanical properties of insulator. A stress value of 11.3 kN/m2 is centred at the FRP Rod and also between the shed and FRP Rod. According to the mechanical displacement analysis, the live end has a displacement of 32mm, whereas the ground end has zero displacement. According to the electric potential analysis the live end has a voltage of 11 kV, whereas zero voltage at the ground end. The electric potential has no effect on the insulator with varying composition of MgO nanofillers, both with and without pollution. But, with increasing distance, the electric potential drops linearly. The electric field has a more significant influence between the metal fitting and the FRP rod connection and has a lower influence at the sheds. It was observed that an insulator with 7.5 percent MgO has better control over the distribution of electric fields. Hence has a positive impact on the insulator's lifespan. Electric Flux Density is low without the pollution layer as compared with pollution layer, demonstrating that electric flux is unaffected by varying the composition of insulators. Leakage current is low for pure SIR and as pollution level rises, the leakage current increases, but as the composition of nanofiller increases, leakage current reduces correspondingly.

REFERENCES

[1] N.Avudaiammal, B.Vigneshwaran and Dr.M.Willjuice Iruthayarajan, "Electric field analysis of 11 kV socket end fitting composite insulator", 10th International Conference on Intelligent Systems and Control, Coimbatore, Tamilnadu, India, Nov 2016. DOI: 10.1109/ISCO.2016.7726899

[2] V.T. Kontargyri, I.F. Gonos, N.C. Ilia And I.A. Stathopulos "Simulation of the Electric Field on Composite Insulators Using the Finite Elements Method", WSEAS Transactions on Circuits and System, pp.1-5, Jan 2014.

[3] El-Sayed M. El-Refaie, M.K. Abd Elrahman and M. Kh. Mohamed, "Electric field distribution of optimized composite insulator profiles under different pollution conditions", Ain Shams Engineering Journal ,Vol 9, Issue 4, pp.1349-1356, Dec 2018.

[4] N. Sumathi and R. Srinivasa Rao, "Seasonal Based Pollution Performance of 11kV and 33kV Silicon Composite Insulators", World Academy of Science, Engineering and Technology International Journal of Energy and Power Engineering, Vol 9, Issue 7, pp.732-737, Jan 2015.

[5] M. Talaat, "Electric Field Simulation Along Silicon Rubber Insulators Surface", 17th International Conference on High Voltage Engineering, Hannover, Germany, pp.1-4, Aug 2011.

[6] B. Marungsri, W. Onchantuek, A. Oonsivilai and T. Kulworawanichpong, "Analysis of Electric Field and Potential Distributions along Surface of Silicon Rubber Insulators under Various Contamination Conditions Using Finite Element Method", World Academy of Science, Engineering and Technology International

Journal of Electrical and Computer Engineering, Vol 3, Issue 5,pp.1237-1247, Feb 2009.

[7] Krishna Patel and B. R. Parekh, "Influence of Design Parameters on Surface Leakage Current of Silicon Rubber Insulator", International Journal of Research in Engineering, Science and Management, Vol 2, Issue 1, pp.116-120, Jan 2019.

[8] Krishal Solanki and Patel Shreyas B, "Comparison of Polymer Insulators using ANSYS 3D simulator and Matlab", International Journal of Advance Engineering and Research development, Vol 5, Issue 09, pp. 422-425, Sept 2018.

[9] N H M Netravati, Sunitha N. S, Dr. Shivakumara Aradhya R.S and Dr. K.N Ravi, "Risk assessment of pollution on a 66kV composite insulator using ANSYS", International Journal of Scientific Development and Research, Vol 1, Issue 11, pp.6-12, Nov 2016.

[10] Haoran Wang, Zongren Peng, Shiling Zhang and Peng Liu, "Simulation Study on E-field Distribution and Corona Characteristics of Composite Insulator with Water Droplets", Conference on Electrical Insulation and Dielectric Phenomena, Chenzhen, China, pp.422-425, Mar 2013.

[11] A.Thabet, M.R.Al-Sharif, Abdel-Moamen.M. A and A.El-Nobi, "Improvement of Electrical Field Distribution on Non-Ceramic Insulators String Using Nanoparticles", 21st International Middle East Power Systems Conference, Cairo, Egypt, pp.195-201, Feb 2020. DOI: 10.1109/MEPCON47431.2019.9008030

[12] Yong Liu, Yafeng Wu and Boxue Du, "Dynamic formation mechanism of water droplet and induced surface discharges on silicon rubber composites", The Institute of Engineering and Technology Digital Library, pp., 8095 – 8101, Vol 7, Mar 2019,DOI: 10.1049/hve.2018.5082.

[13] Sounak Nandi and Subba Reddy B, "Transient Electric Field Analysis for Polluted Composite Insulators under HVDC stress", IEEE Transactions on Power Delivery, Vol 36, Issue 2, pp.1-11, April 2020, DOI 10.1109/TPWRD.2020.2987143.

[14] Sounak Nandi, B. Subba Reddy and Dinesh Sharma, "Performance of Composite Insulators Used for Electric Transmission under Extreme Climatic Conditions", Journal of Materials Engineering and Performance, Sept 2019.

[15] Kavyashree C. M and Shilpa S. K, "Electric Stress Analysis of 132 kV Composite Long Rod Insulator", International Journal of Science and Research, Vol 5, Issue 5, pp.1001-1004, May 2016.